



1 **Investigation of water adsorption and hygroscopicity of atmospheric**
2 **particles using a commercial vapor sorption analyzer**

3

4 Wenjun Gu^{1,4}, Yongjie Li², Jianxi Zhu³, Xiaohong Jia^{1,4}, Qin hao Lin¹, Guohua Zhang¹, Xiang
5 Ding¹, Wei Song¹, Xinhui Bi¹, Xinming Wang^{1,5}, Mingjin Tang^{1,*}

6

7 1 State Key Laboratory of Organic Geochemistry and Guangdong Key Laboratory of
8 Environmental Protection and Resources Utilization, Guangzhou Institute of Geochemistry,
9 Chinese Academy of Sciences, Guangzhou 510640, China

10 2 Department of Civil and Environmental Engineering, Faculty of Science and Technology,
11 University of Macau, Avenida da Universidade, Taipa, Macau, China

12 3 CAS Key Laboratory of Mineralogy and Metallogeny and Guangdong Provincial Key
13 Laboratory of Mineral Physics and Material Research & Development, Guangzhou Institute of
14 Geochemistry, Chinese Academy of Sciences, Guangzhou 510640, China

15 4 University of Chinese Academy of Sciences, Beijing 100049, China

16 5 Center for Excellence in Regional Atmospheric Environment, Institute of Urban
17 Environment, Chinese Academy of Sciences, Xiamen 361021, China

18

19 Correspondence: M. J. Tang (Email: mingjintang@gig.ac.cn)

20



21 **Abstract**

22 Water adsorption and hygroscopicity are among the most important physicochemical
23 properties of aerosol particles, largely determining their impacts on atmospheric chemistry,
24 radiative forcing, and climate. Measurements of water adsorption and hygroscopicity of
25 nonspherical particles under subsaturation conditions are non-trivial because many widely used
26 techniques require the assumption of particle sphericity. In this work we describe a method to
27 directly quantify water adsorption and mass hygroscopic growth of atmospheric particles for
28 temperature in the range of 5-30 °C, using a commercial vapor sorption analyzer. A detailed
29 description of instrumental configuration and experimental procedures, including relative
30 humidity (RH) calibration, are provided first. It is then demonstrated that for (NH₄)₂SO₄ and
31 NaCl, deliquescence relative humidities (DRHs) and mass hygroscopic growth factors
32 measured using this method show good agreements with experimental and/or theoretical data
33 from literature. To illustrate its ability to measure water uptake by particles with low
34 hygroscopicity, we used this instrument to investigate water adsorption by CaSO₄·2H₂O as a
35 function of RH at 25 °C. The mass hygroscopic growth factor of CaSO₄·2H₂O at 95% RH,
36 relative to that under dry conditions (RH < 1%), was determined to be (0.450±0.004)% (1 σ).
37 In addition, it is shown that this instrument can reliably measure a relative mass change of
38 0.025%. Overall, we have demonstrated that this commercial instrument provides a simple,
39 sensitive, and robust method to investigate water adsorption and hygroscopicity of atmospheric
40 particles.

41



42 **1 Introduction**

43 Atmospheric aerosol particles, directly emitted by natural and anthropogenic processes or
44 secondarily formed in the atmosphere, have significant impacts on air quality, visibility, human
45 health, and radiative and energy balance of the Earth system (Pöschl, 2005; Seinfeld and Pandis,
46 2006). The ability to uptake water is among the most important physicochemical properties of
47 aerosol particles, and it largely determines their impacts on atmospheric chemistry and climate
48 (Martin, 2000; Rubasinghege and Grassian, 2013; Farmer et al., 2015; Tang et al., 2016). The
49 ability of aerosol particles to uptake water depends on particle composition, relative humidity
50 (RH), and temperature (Martin, 2000; Tang et al., 2016). Under subsaturation conditions (RH
51 <100%), the ability to uptake water is typically called water adsorption in surface science and
52 hygroscopicity in aerosol science (Tang et al., 2016). Under supersaturation conditions, aerosol
53 particles can be activated to cloud droplets (McFiggans et al., 2006; Petters and Kreidenweis,
54 2007) and ice particles if temperature is below 0 °C (Pruppacher and Klett, 1994; Vali et al.,
55 2015).

56 Hygroscopicity of atmospheric particles has been extensively investigated by a large
57 number of studies, and many experimental techniques have been developed. These techniques
58 have been summarized and discussed by a very recent review paper (Tang et al., 2016), and
59 here we only mention widely used ones. For airborne monodisperse particles typically
60 produced by a differential mobility analyzer (DMA), the hygroscopicity can be determined by
61 measuring their diameters at dry (typically at RH <15% or lower) and humidified conditions
62 (Swietlicki et al., 2008; Freedman et al., 2009; Robinson et al., 2013; Lei et al., 2014). Typically,
63 the diameter change is determined by using a scanning particle mobility sizer (in which
64 mobility diameters are measured) (Vlasenko et al., 2005; Swietlicki et al., 2008; Herich et al.,
65 2009; Koehler et al., 2009; Wu et al., 2011) or aerosol extinction-cavity ring down
66 spectrometry (in which optical diameters are measured) (Freedman et al., 2009; Attwood and



67 Greenslade, 2011). These techniques require an underlying assumption that particles are
68 spherical. However, a few important types of particles in the troposphere, including mineral
69 dust and soot, are known to be non-spherical (Veghte and Freedman, 2012; Ardon-Dryer et al.,
70 2015). Therefore, although these techniques can provide useful information, it is difficult to
71 quantitatively determine the amounts of water associated with non-spherical particles at a given
72 RH (Tang et al., 2016). Single particle levitation techniques, which measure light scattering
73 intensity to determine the size (and thus the hygroscopic growth) of levitated particles, also
74 have similar drawbacks (Krieger et al., 2012).

75 There are several techniques which can be applied to quantify the amount of water
76 associated with non-spherical particles at given temperature and RH. For example, adsorbed
77 water can be measured by FTIR by its IR absorption at around 3400 and 1645 cm^{-1} (Goodman
78 et al., 2001; Frinak et al., 2005; Ma et al., 2010a). However, it is non-trivial to convert IR
79 absorption intensity to the amount of adsorbed water (Schuttlefield et al., 2007a; Tang et al.,
80 2016). Several previous studies have used quartz crystal microbalance (QCM) to measure DRH
81 and mass hygroscopic growth of particles (Schuttlefield et al., 2007b; Arenas et al., 2012; Liu
82 et al., 2016; Yeşilbaş and Boily, 2016). The frequency change of the quartz crystal in a QCM,
83 according to the Sauerbrey equation, is proportional to the change in mass of particles loaded
84 on the crystal (Schuttlefield et al., 2007b). In addition, the amount of water associated with
85 particles at a given RH can also be determined by measuring the change in water vapor pressure
86 before and after exposure of particles to water vapor (Ma et al., 2010b; Ma et al., 2012), in a
87 manner similar to determination of Brunauer-Emmett-Teller surface area. In theory the
88 electrodynamic balance can be used to investigate the mass hygroscopic growth of non-
89 spherical particles (Chan et al., 2008; Lee et al., 2008; Pope, 2010; Griffiths et al., 2012). To
90 our knowledge, however, this technique has not been applied to mineral dust and soot particles
91 yet.



92 In this work we have developed an experimental method to investigate water adsorption
93 and hygroscopicity of atmospheric particles, using a vapor sorption analyzer which is
94 commercially available. We note that two groups have used similar techniques to measure
95 water adsorption by CaCO_3 and Arizona Test dust (Gustafsson et al., 2005) and DRH of
96 malonic acid, sodium oxalate, and sodium malonate (Beyer et al., 2014; Schroeder and Beyer,
97 2016). Nevertheless, the performance of this technique has never been systematically evaluated.
98 To validate this experimental method, we have determined DRHs of six compounds as a
99 function of temperature from 5 to 30 °C, and the measured DRHs, varying from ~20% to ~90%
100 RH, show excellent agreement with literature values. In addition, mass hygroscopic growth
101 factors (MGF) of $(\text{NH}_4)_2\text{SO}_4$ and NaCl have been measured as a function of RH at 25 and 5 °C,
102 and the measured MGF agree very well with those predicted by the E-AIM model
103 (<http://www.aim.env.uea.ac.uk/aim/aim.php>; last accessed: 11 January 2016). We show that
104 this instrument can measure a relative mass change (due to water uptake) of <0.025% within 6
105 hours and <0.05% within 24 hours, and the accuracy of mass change measurement is mainly
106 limited by baseline drifts. These features make this instrument particularly useful for laboratory
107 studies of water adsorption by nonspherical particles and/or particles with low hygroscopicity.

108 **2 Experimental section**

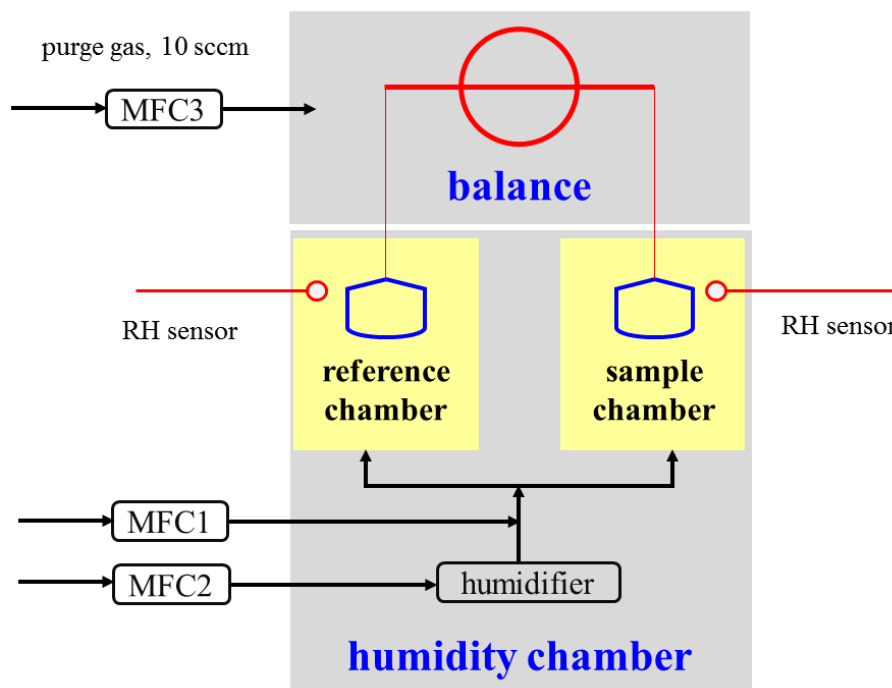
109 The instrument used in this work is a vapour sorption analyser (Q5000SA) manufactured
110 by TA Instruments (New Castle, DE, USA). The first part of this section provides a general
111 description of this instrument, and the second part describes experimental methods used in this
112 work.

113 **2.1 Instrument description**

114 Figure 1 shows the schematic diagram of the vapor sorption analyzer used in this work to
115 measure hygroscopicity and water adsorption of particles of atmospheric relevance. This
116 instrument consists of two main parts: 1) a high-precision balance used to measure the mass of



117 samples; 2) a humidity chamber in which temperature and RH can be precisely regulated and
118 accurately monitored online.



119

120 **Figure 1.** Schematic diagram of Q5000SA used in this work. MFC: mass flow controller. High
121 purity N₂ is used for all the three gas flows regulated by MFC1, MFC2, and MFC3, respectively.

122 2.1.1 High-precision balance

123 The balance simultaneously measures the mass of an empty pan (serving as a reference)
124 and a sample pan which contains particles under investigation. Each pan is connected to the
125 balance by a hang-down wire which has a hook at the lower end to hold the pan. The balance
126 is housed in a chamber which is temperature regulated. To avoid moisture condensation, the
127 balance chamber is purged with a 10 sccm (standard cubic centimetre per min) N₂ flow
128 regulated by a mass flow controller (MFC3).

129 The balance has a dynamic range of 0-100 mg. Typical dry mass of particles used in our
130 experiments are around 10 mg or less so that the total mass of particles due to adsorption of



131 water at high RH does not exceed the upper limit of the balance. The stated sensitivity of the
132 balance is $<0.1 \mu\text{g}$ with a weighing accuracy of $\pm 0.1\%$, a weighing precision of $\pm 0.01\%$, and a
133 signal resolution of $<0.01 \mu\text{g}$. The 24-h baseline drift is stated to be $<5 \mu\text{g}$ for an empty
134 metalized quartz pan at $25 \text{ }^\circ\text{C}$ and $20\% \text{ RH}$. This is equivalent to a relative mass change of
135 $<0.05\%$ if the sample mass is 10 mg . As shown Section 3.3, experimental tests do suggest that
136 such performance can be reached.

137 **2.1.2 Humidity chamber**

138 The humidity chamber is used to regulate the temperature and RH under which
139 hygroscopicity and/or water adsorption of particles are investigated. Inside the humidity
140 chamber are housed a reference chamber (in which an empty pan is connected to the balance)
141 and a sample chamber (in which a sample pan is connected to the balance). A dry N_2 flow
142 (regulated by MFC2) is delivered through a humidifier and then mixed the second dry N_2 flow
143 (regulated by MFC1). The total flow is set to 200 sccm , and the ratio of these two flows can be
144 adjusted in order to regulate the final RH. After mixing, the flow is then split into two flows,
145 one delivered into the reference chamber and the other into the sample chamber. Therefore,
146 both chambers should have the same temperature and RH. This can be verified by
147 measurements using two RH sensors, as shown in Figure 1. The main advantage of using a
148 reference chamber and a sample chamber is that the amount of water adsorbed by the empty
149 pan and the attached wire can be simultaneously determined (and automatically subtracted
150 using the provided software) under the same condition when water uptake by particles under
151 investigation is being measured. In addition, the effect of buoyancy, which varies with RH
152 (Beyer et al., 2014; Schroeder and Beyer, 2016), is also automatically taken into account by
153 using an empty pan as the reference.

154 Temperature inside the humidity chamber can be adjusted from 5 to $85 \text{ }^\circ\text{C}$ with a stated
155 stability of $\pm 0.1 \text{ }^\circ\text{C}$, and RH can be varied between 0 and 98% , with an absolute accuracy of



156 $\pm 1\%$. Semispherical quartz crucibles with a volume of 180 μL , provided by the manufacturer,
157 are used in this work as sample pans.

158 **2.1.3 Other features**

159 Q5000SA is equipped with a programmable autosampler designed to deliver sample pans
160 into the humidity chamber. The autosampler can host up to 10 sample pans; however, in order
161 to minimize contamination by lab air, only one sample pan is uploaded into the autosampler
162 immediately prior to the measurement. The instrument status is displayed on a touch screen for
163 local operation. Q5000SA can also communicate with a computer via Ethernet. Two software
164 packages are provided by the manufacturer: 1) TA Instrument Explorer Q Series is used to
165 control the instrument, program measurement procedures, and log experimental data; 2) TA
166 Universal Analysis can be used for graphing experimental data in real time, data analysis, and
167 exporting data. Experimental data can be sampled with frequencies up to 1 Hz.

168 **2.2 Experimental procedures**

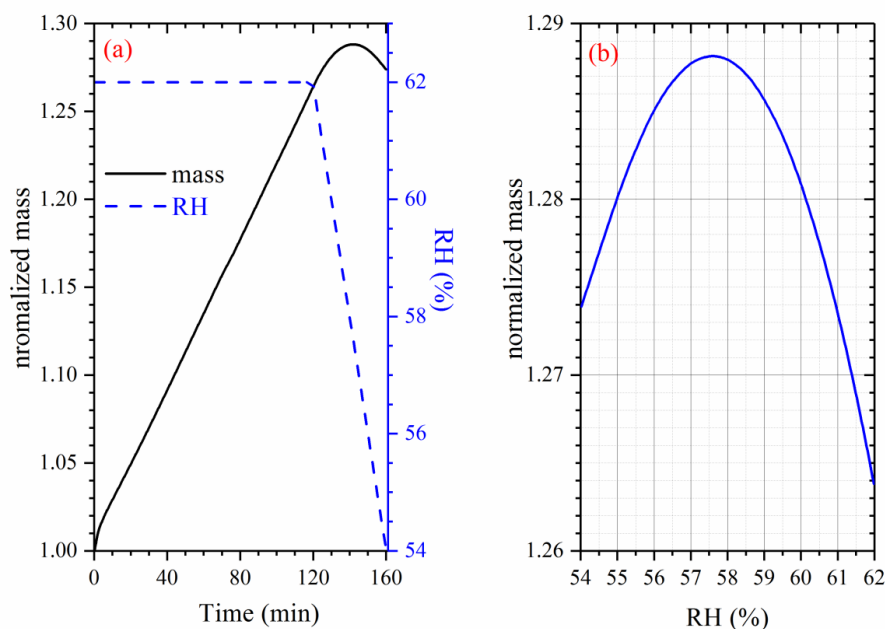
169 In our work two major experimental protocols are developed to 1) determine the DRH and
170 2) quantify water adsorption and/or mass hygroscopic growth. Corresponding experimental
171 procedures are detailed below.

172 **2.2.1 DRH determination**

173 Based on the standard recommended by American Society for Testing and Materials
174 International (ASTM, 2007) and TA Instruments (Waguespack and Hesse, 2007), an
175 experimental method has been developed in this work to determine the DRH of a given sample.
176 It consists of the following three major steps: 1) after the sample pan is properly located in the
177 humidity chamber, temperature is set to the given value; 2) after temperature is stabilized, RH
178 is set to a value which is $\sim 5\%$ (when change/difference in RH is mentioned in this work, it
179 always means the absolute value) higher than the anticipated DRH and the system is



180 equilibrated for 120 min; 3) RH is linearly decreased with a rate of 0.2% per min to a value
181 which is ~5% lower than the anticipated DRH.



182

183 **Figure 2.** Typical experimental data in determination of DRH at a given temperature (NaBr at
184 25 °C as an example) using Q5000SA by linearly decreasing RH. (a): Change of normalized
185 sample mass (solid curve, left y-axis) and RH (dashed curve, right y-axis) as a function of time;
186 (b): Change of normalized sample mass as a function of RH when RH decreased linearly from
187 62% to 54%.

188

189 Figure 2a shows changes of RH and sample mass (normalized to that at 0 min) as a function
190 of time in an experiment to measure the DRH of NaBr at 25 °C. RH was kept at 62% in the
191 first 120 min during which the sample mass increased with time. After that, RH was linearly
192 decreased to 54% with a rate of 0.2% RH per min, and during this period the sample mass first
193 continued to increase to a maximum value and then decreased with time. The sample mass in



194 the second period (120-160 min, as shown in Figure 2a) is plotted as a function of RH, and the
195 RH (57.6% in this case) at which the sample mass reached the maximum value is equal to the
196 measured DRH (ASTM, 2007).

197 Measurement of a DRH usually takes ~3 h in total, and experimental data such as RH and
198 sample mass are recorded with a time resolution of 10 s. If the DRH is unknown, we can
199 increase the upper RH and decrease the lower RH used in the measurement so that the DRH
200 falls into the RH range. Increasing RH range used in the measurement will of course lead to
201 the increase of experimental time required.

202 **2.2.2 Quantification of water adsorption and/or mass hygroscopic growth**

203 The following experimental procedures are used to determine the amount of water
204 adsorbed by a material (i.e. mass hygroscopic growth factors): 1) a sample pan is delivered into
205 the humidity chamber and temperature in the humidity chamber is set to a given value; 2) after
206 temperature becomes stable, RH in the humidity chamber is set to 0% and the sample is
207 equilibrated with the environment until its mass change is <0.05% within 30 min; 3) RH is
208 increased to a given value and the sample is equilibrated with the environment again until its
209 mass change is smaller than a certain value (typically 0.05% for less hygroscopic materials
210 such as CaCO₃ and fresh soot, and 0.1% for more hygroscopic materials such as (NH₄)₂SO₄
211 and NaCl) within 30 min; 4) RH is further increased to another given value and the sample is
212 equilibrated with the environment. The following assumptions are made to convert the mass of
213 adsorbed water to its surface coverage (Tang et al., 2016): 1) particles are spherical, having a
214 uniform diameter of 1 μm and a density of 2.5 g cm⁻³, and 2) the average surface area that an
215 adsorbed water molecule occupies is 1×10⁻¹⁵ cm². Under these assumptions, a mass change of
216 0.05% (relative to the dry mass) due to adsorption of water is equal to a surface coverage of
217 0.7 monolayers for adsorbed water.



218 All the processes are programmed, with the flexibility to choose the number of RH steps
219 and the corresponding RH values. Experimental data such as RH and sample mass are recorded
220 with a time resolution of 30 s. Relevant experimental results will be presented in detail in
221 Sections 3.3 and 3.4.

222 **2.3 Chemicals**

223 Sodium bromide, provided by TA Instruments as a reference material for RH calibration,
224 was supplied by Alfa Aesar with a stated purity of >99.7%. Ammonium sulfate
225 (purity: >99.0%), sodium chloride (purity: >99.5%), potassium chloride (purity: >99.5%),
226 magnesium nitrate hexahydrate (purity: >99.0%), magnesium chloride hexahydrate
227 (purity: >99.0%), calcium bromide (purity: >99.98%), and calcium sulfate dihydrate
228 (purity: >99%) were purchased from Sigma-Aldrich. All the chemicals were used without
229 further pretreatment.

230 **3 Results and Discussion**

231 **3.1 RH calibration**

232 RH in the humidity chamber is measured by two RH sensors, as shown in Figure 1. RH
233 measurements of vapor sorption analyzers and/or thermogravimetric analyzers can be
234 calibrated/verified by determining the DRH of a reference material with a well-defined DRH
235 (ASTM, 2007). In this work, NaBr provided by TA Instruments is used as the reference
236 material (Waguespack and Hesse, 2007). We compare our measured DRHs of NaBr at six
237 different temperatures with those reported by a previous study (Greenspan, 1977). The results
238 are summarized in Table 1, suggesting that the differences between our measured and previous
239 reported DRHs is <1% RH for temperatures ranging from 5 to 30 °C. The agreement is
240 excellent, especially considering that 1) the stated RH measurement of our instrument has an
241 accuracy of $\pm 1\%$ and 2) DRH values reported by Greenspan (1977) typically have errors of



242 $\pm 0.5\%$. Further inspection of results compiled in Table 1 reveals that the difference is larger at
243 lower temperature and becomes smaller at higher temperature.

244

245 **Table 1.** Comparison of DRHs (in %) of NaBr at different temperatures measured in our
246 study with those reported in literature (Greenspan, 1977).

T (°C)	5	10	15	20	25	30
DRH (literature)	63.5 \pm 0.7	62.2 \pm 0.6	60.7 \pm 0.5	59.1 \pm 0.4	57.6 \pm 0.4	56.0 \pm 0.4
DRH (this work)	62.2	61.2	60.0	58.5	57.6	56.1
difference in DRH	1.3	1.0	0.7	0.6	0.0	-0.1

247

248 DRH values reported by Greenspan (1977), widely accepted as standard values, are
249 recommended by the instrument manufacturer (Waguespack and Hesse, 2007) and also used
250 in this study to calibrate our measure RH by taking into account the difference between our
251 measured DRHs and those reported by Greenspan (1977) for NaBr at different temperatures.
252 All the RHs reported in this work (except measured DRHs of NaBr listed in Table 1) have been
253 calibrated. In our work we have not verified RH measurements for temperature higher than 30
254 °C because the atmospheric relevance is limited. It should be pointed out if necessary, RH
255 calibration can also be carried out at higher temperature (up to 85 °C) using the same procedure.

256 3.2 DRH measurements

257 Using the experimental method detailed in Section 2.2.1, we have measured DRHs of
258 CaBr₂, MgCl₂·6H₂O, Mg(NO₃)₂·6H₂O, NaCl, (NH₄)₂SO₄, and KCl at different temperatures
259 from 5 to 30 °C. All the experimental results are summarized in Table 2. Figure 3a display our
260 measured DRHs of these compounds at 25 °C. DRHs range from ~20% to almost 90% for these
261 six compounds. As evident from Figure 3a, our measured DRHs show excellent agreement
262 with those reported by a previous study (Greenspan, 1977). Figure 3b shows the comparison
263 of our measured DRHs with those reported in literature for Mg(NO₃)₂·6H₂O as a function of



264 temperature (5-30 °C), and excellent agreement is found again. Careful examination of data
 265 compiled in Table 2 suggests that the absolute difference between our measured and previously
 266 reported DRHs is typically <1%.

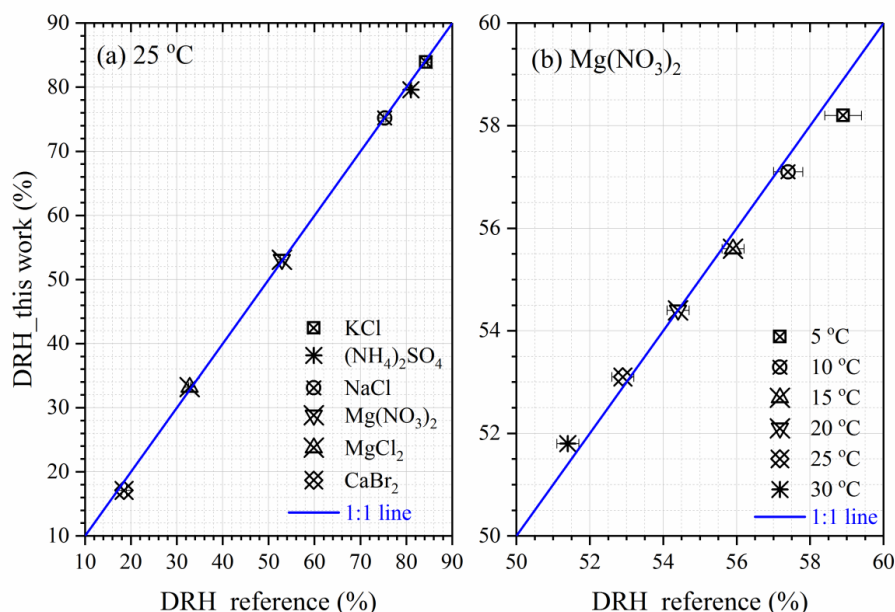
267

268 **Table 2.** Comparison of DRHs measured by our study with those reported in literature
 269 (Greenspan, 1977) for CaBr₂, MgCl₂·6H₂O, Mg(NO₃)₂·6H₂O, NaCl, (NH₄)₂SO₄, and KCl from
 270 5-30 °C. NA: data are not available.

T (°C)	literature	this work	literature	this work	literature	this work
	CaBr ₂		MgCl ₂ ·6H ₂ O		Mg(NO ₃) ₂ ·6H ₂ O	
5	NA	22.9	33.6±0.3	33.3	58.9±0.5	58.2
10	21.6±0.5	21.6	33.5±0.3	33.9	57.4±0.4	57.1
15	20.2±0.5	20.0	33.3±0.3	33.6	55.9±0.3	55.6
20	18.5±0.5	18.0	33.1±0.2	33.5	54.4±0.3	54.4
25	18.5±0.5	17.1	32.8±0.2	33.2	52.9±0.3	53.1
30	NA	17.7	32.4±0.2	33.6	51.4±0.3	51.8
	NaCl		(NH ₄) ₂ SO ₄		KCl	
5	75.6±0.5	76.0	82.4±0.7	80.8	87.7±0.5	86.7
10	75.7±0.4	75.7	82.1±0.5	80.8	86.8±0.4	86.3
15	75.6±0.3	75.7	81.7±0.4	80.4	85.9±0.4	85.6
20	75.5±0.3	75.6	81.3±0.3	80.3	85.1±0.3	85.0
25	75.3±0.3	75.2	81.0±0.3	79.6	84.3±0.3	83.9
30	75.1±0.3	75.5	80.6±0.3	79.7	83.6±0.3	83.4

271

272 In addition, we repeated the measurements of the DRH of (NH₄)₂SO₄ at 25 °C on different
 273 days, and in total eight measurements have been carried out. The measured DRHs range from
 274 79.5% to 80.1%. Therefore, it can be concluded from our systematical tests that the
 275 experimental method developed in our work can reliably measure DRHs from 5 to 30 °C.



276

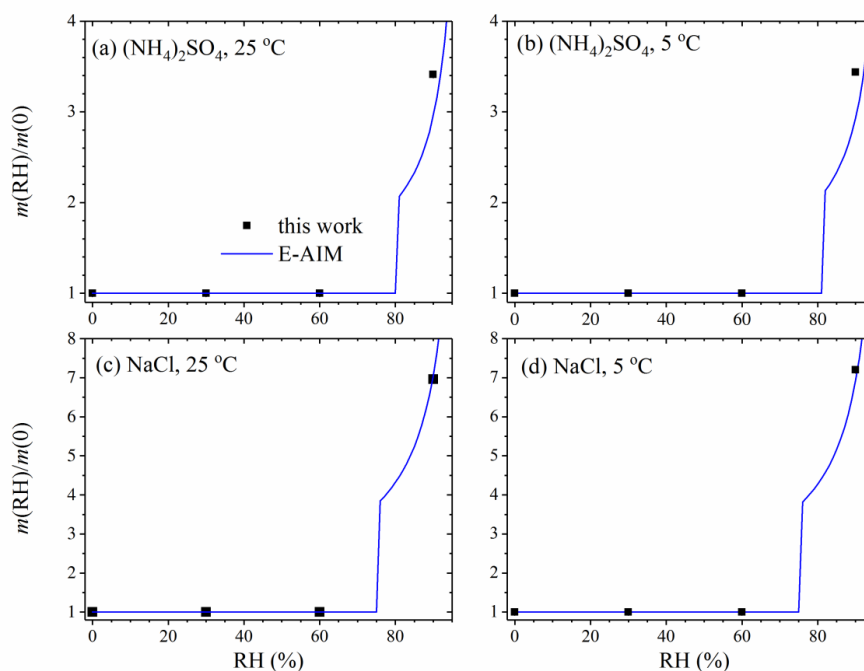
277 **Figure 3.** Comparison of our measured and previous reported DRHs (Greenspan, 1977). (a)
278 DRHs of (NH₄)₂SO₄, NaCl, MgCl₂·6H₂O, Mg(NO₃)₂·6H₂O, CaBr₂, and KCl at 25 °C; (b)
279 DRHs of Mg(NO₃)₂·6H₂O as a function of temperature from 5-30 °C.

280 3.3 Mass hygroscopic growth measurements

281 (NH₄)₂SO₄ and NaCl are important components found in tropospheric aerosol particles,
282 and their hygroscopicity has been well understood. They have also been widely used as
283 standard materials for validation of hygroscopicity and cloud condensation nucleation activity
284 measurements (Good et al., 2010; Ma et al., 2010b; Tang et al., 2015). In our work we have
285 measured mass hygroscopic growth factors of (NH₄)₂SO₄ and NaCl as a function of RH (0%,
286 30%, 60%, and 90%) at two different temperatures, with the purpose to further assess the
287 performance of our new method. Figure 4 show the comparison of mass hygroscopic growth
288 factors measured by our work with those predicted by the E-AIM model (Wexler and Clegg,
289 2002). It can be concluded from the comparison that our measured mass hygroscopic growth
290 factors agree well with theoretical values for (NH₄)₂SO₄ and NaCl at both 5 and 25 °C. This



291 gives us further confidence that the method developed in this work is reliable for
292 hygroscopicity measurements of atmospheric particles.



293

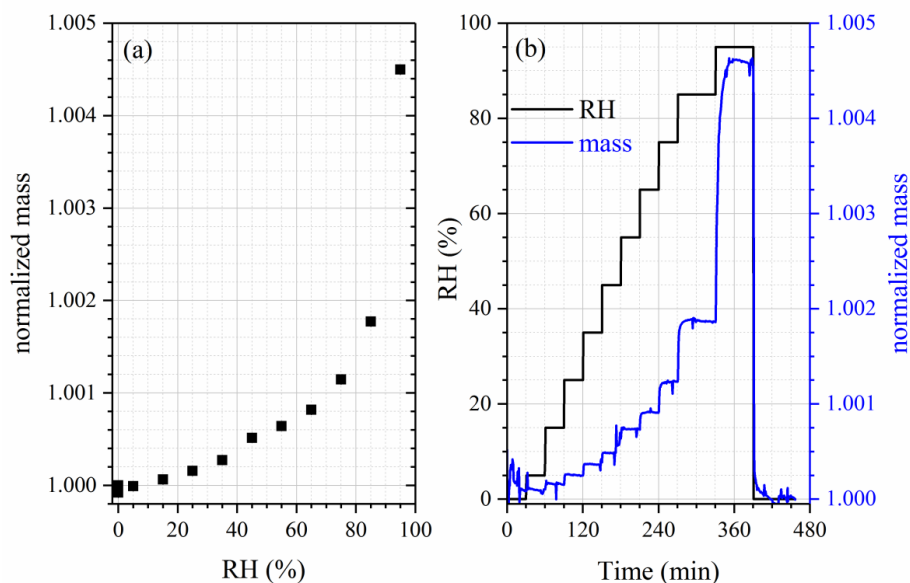
294 **Figure 4.** Comparison of mass hygroscopic growth factors measured in this work with these
295 predicted by the E-AIM model. (a) $(\text{NH}_4)_2\text{SO}_4$ at 5 °C; (b) $(\text{NH}_4)_2\text{SO}_4$ at 25 °C; (c) NaCl at
296 25 °C; (d) NaCl at 5 °C.

297

298 We have also measured the mass hygroscopic growth factors of $\text{CaSO}_4 \cdot 2\text{H}_2\text{O}$ as a function
299 of RH (up to 95%) at 25 °C. The results are plotted in Figure 5a, and the numerical data are
300 summarized in the appendix (Table A1). As shown in Figure 5, the ability of $\text{CaSO}_4 \cdot 2\text{H}_2\text{O}$ to
301 uptake water is very limited, with the mass ratio of adsorbed water to dry particles is
302 $(0.450 \pm 0.004)\%$ (1σ) at 95% RH. This is qualitatively consistent with two previous studies
303 which suggested that the cloud condensation nucleation activity of calcium sulfate aerosol



304 particles is very low (Sullivan et al., 2009b; Tang et al., 2015). More detailed comparison and
305 discussion are beyond the scope of this paper and will be addressed in a following publication.



306
307 **Figure 5.** (a) Measured mass hygroscopic growth factors (normalized to the mass at 0% RH)
308 of $\text{CaSO}_4 \cdot 2\text{H}_2\text{O}$ as a function of RH up to 95% RH. (b) Time series of RH and normalized mass
309 of $\text{CaSO}_4 \cdot 2\text{H}_2\text{O}$ particles with a dry mass of ~ 9.05 mg during a hygroscopic growth experiment.
310 This experiment was carried out at 25 °C.

311
312 Figure 5b displays change of RH and normalized sample mass with time during the
313 measurement, suggesting that within 6 h our method can measure a relative mass change of
314 $< 0.25\%$. The accuracy of mass measurement is mainly limited by long-term baseline drifts. In
315 another experiment, a CaCO_3 sample (with a dry mass of ~ 10 mg) was used, and its mass was
316 continuously monitored under dry conditions at 25 °C. Under this experimental condition, the
317 baseline drift was determined to be $< 0.05\%$ within 24 h.



318 **4. Conclusion and outlook**

319 The ability to uptake water vapor under sub-saturation conditions is one of the most
320 important physicochemical properties of atmospheric particles, largely determining their
321 impacts on atmospheric chemistry and climate. In this work, we have developed a new
322 experimental method to investigate interactions of particles with water vapor under sub-
323 saturation conditions at different temperatures from 5 to 30 °C, using a commercial vapor
324 sorption analyzer. Operation temperature can be increased up to 85 °C, though the atmospheric
325 relevance is limited. We have provided a detailed description of instrument configuration as
326 well as experimental procedures to determine DRHs and mass hygroscopic growth factors. For
327 the temperature range we have covered in this work (5-30 °C), our measured DRHs of six
328 different compounds with DRHs ranging from ~20% to ~90%, show excellent agreement with
329 those reported in literature. In addition, mass hygroscopic growth factors measured in our work
330 at different RH values agree well with those predicted by the E-AIM model for (NH₄)₂SO₄ and
331 NaCl at 5 and 25 °C. Therefore, we have demonstrated that experimental methods developed
332 in our work can reliably measure DRHs and mass hygroscopic growth factors from 5 to 30 °C.

333 To test the ability of this instrument to measure hygroscopic growth of compounds with
334 low hygroscopicity, we have determined mass hygroscopic growth factors of CaSO₄·2H₂O at
335 25 °C. It has been found that the ability of CaSO₄·2H₂O to uptake water is very limited. The
336 mass of water adsorbed by CaSO₄·2H₂O at 95% RH is only (0.450±0.004)% of its dry mass. It
337 has also been observed that this instrument can measure a mass change of <0.025% within 6
338 hours and <0.05% within 24 h, and accuracy of mass change determination is mainly limited
339 by baseline drifts. With such an accuracy, this instrument is particularly useful for quantitative
340 determination of water adsorption and/or hygroscopicity of non-spherical particles such as
341 mineral dust and soot. Atmospheric aging processes are known to alter water adsorption,
342 hygroscopicity, and cloud condensation nucleation activity of mineral dust and soot particles



343 (Kelly and Wexler, 2005; Laskin et al., 2005; Zhang et al., 2008; Sullivan et al., 2009a; Han et
344 al., 2013; Denjean et al., 2015; Tang et al., 2016). In the future, this instrument will be used to
345 investigate water adsorption and hygroscopicity of mineral dust and soot particles before and
346 after chemical processing.

347

348 **Data availability**

349 Experimental data presented in this work are available upon request (Mingjin Tang:
350 mingjintang@gig.ac.cn).

351

352 **Acknowledgement**

353 Financial support provided by Chinese National Science Foundation (grant No.: 41675120),
354 Chinese Academy of Sciences international collaborative project, and State Key Laboratory of
355 Organic Geochemistry (grant No.: SKLOGA201603A) is acknowledged. Mingjin Tang would
356 like to thank the CAS Pioneer Hundred Talents program for providing a starting grant and
357 Yongjie Li would like to acknowledge funding support of the Start-up Research Grant from
358 University of Macau (SRG2015-00052-FST). The authors declare no competing financial
359 interest.

360

361 **Appendix**

362 **Table A1.** Normalized mass of $\text{CaSO}_4 \cdot 2\text{H}_2\text{O}$ as a function of RH at 25 °C.

RH (%)	0	5	15	25	35	45
normalized mass	1.00000	0.99999	1.00006	1.00016	1.00027	1.00051
Error	0.00001	0.00002	0.00001	0.00001	0.00004	0.00005
RH (%)	55	65	75	85	95	0
normalized mass	1.00064	1.00082	1.00114	1.00177	1.00450	0.99992
error	0.00002	0.00001	0.00001	0.00001	0.00004	0.00001

363



364 **References:**

- 365 Ardon-Dryer, K., Garimella, S., Huang, Y. W., Christopoulos, C., and Cziczo, D. J.:
366 Evaluation of DMA Size Selection of Dry Dispersed Mineral Dust Particles, *Aerosol Sci.*
367 *Technol.*, 49, 828-841, 2015.
- 368 Arenas, K. J. L., Schill, S. R., Malla, A., and Hudson, P. K.: Deliquescence Phase Transition
369 Measurements by Quartz Crystal Microbalance Frequency Shifts, *J. Phys. Chem. A*, 116,
370 7658-7667, 2012.
- 371 ASTM: Standard Test Method for Humidity Calibration (or Conformation) of Humidity
372 Generators for Use with Thermogravimetric Analyzers, American Society for Testing and
373 Materials International, West Conshohocken, PA 19428, USA, doi: 10.1520/E2551-1507,
374 2007.
- 375 Attwood, A. R., and Greenslade, M. E.: Optical Properties and Associated Hygroscopicity of
376 Clay Aerosols, *Aerosol Sci. Technol.*, 45, 1350-1359, 2011.
- 377 Beyer, K. D., Schroeder, J. R., and Kissinger, J. A.: Temperature-Dependent Deliquescence
378 Relative Humidities and Water Activities Using Humidity Controlled Thermogravimetric
379 Analysis with Application to Malonic Acid, *J. Phys. Chem. A*, 118, 2488-2497, 2014.
- 380 Chan, M. N., Kreidenweis, S. M., and Chan, C. K.: Measurements of the hygroscopic and
381 deliquescence properties of organic compounds of different solubilities in water and their
382 relationship with cloud condensation nuclei activities, *Environ. Sci. Technol.*, 42, 3602-3608,
383 2008.
- 384 Denjean, C., Caquineau, S., Desboeufs, K., Laurent, B., Maille, M., Quiñones Rosado, M.,
385 Vallejo, P., Mayol-Bracero, O. L., and Formenti, P.: Long-range transport across the Atlantic
386 in summertime does not enhance the hygroscopicity of African mineral dust, *Geophys. Res.*
387 *Lett.*, 42, 7835-7843, 2015.
- 388 Farmer, D. K., Cappa, C. D., and Kreidenweis, S. M.: Atmospheric Processes and Their
389 Controlling Influence on Cloud Condensation Nuclei Activity, *Chem. Rev.*, 115, 4199-4217,
390 2015.
- 391 Freedman, M. A., Hasenkopf, C. A., Beaver, M. R., and Tolbert, M. A.: Optical Properties of
392 Internally Mixed Aerosol Particles Composed of Dicarboxylic Acids and Ammonium
393 Sulfate, *J. Phys. Chem. A*, 113, 13584-13592, 2009.
- 394 Frinak, E. K., Mashburn, C. D., Tolbert, M. A., and Toon, O. B.: Infrared characterization of
395 water uptake by low-temperature Na-montmorillonite: Implications for Earth and Mars, *J.*
396 *Geophys. Res.-Atmos.*, 110, D09308, doi: 09310.01029/02004JD005647, 2005.
- 397 Good, N., Coe, H., and McFiggans, G.: Instrumentational operation and analytical
398 methodology for the reconciliation of aerosol water uptake under sub- and supersaturated
399 conditions, *Atmos. Meas. Tech.*, 3, 1241-1254, 2010.
- 400 Goodman, A. L., Bernard, E. T., and Grassian, V. H.: Spectroscopic Study of Nitric Acid and
401 Water Adsorption on Oxide Particles: Enhanced Nitric Acid Uptake Kinetics in the Presence
402 of Adsorbed Water, *J. Phys. Chem. A*, 105, 6443-6457, 2001.
- 403 Greenspan, L.: Humidity fixed points of binary saturated aqueous solutions, *J. Res. Nbs.-A.*
404 *Phys. Chem.*, 81, 89-96, 1977.
- 405 Griffiths, P. T., Borlace, J. S., Gallimore, P. J., Kalberer, M., Herzog, M., and Pope, F. D.:
406 Hygroscopic growth and cloud activation of pollen: a laboratory and modelling study, *Atmos.*
407 *Sci. Lett.*, 13, 289-295, 2012.
- 408 Gustafsson, R. J., Orlov, A., Badger, C. L., Griffiths, P. T., Cox, R. A., and Lambert, R. M.:
409 A comprehensive evaluation of water uptake on atmospherically relevant mineral surfaces:
410 DRIFT spectroscopy, thermogravimetric analysis and aerosol growth measurements, *Atmos.*
411 *Chem. Phys.*, 5, 3415-3421, 2005.



- 412 Han, C., Liu, Y. C., and He, H.: Heterogeneous photochemical aging of soot by NO₂ under
413 simulated sunlight, *Atmos. Environ.*, 64, 270-276, 2013.
- 414 Herich, H., Tritscher, T., Wiacek, A., Gysel, M., Weingartner, E., Lohmann, U.,
415 Baltensperger, U., and Cziczo, D. J.: Water uptake of clay and desert dust aerosol particles at
416 sub- and supersaturated water vapor conditions, *Phys. Chem. Chem. Phys.*, 11, 7804-7809,
417 2009.
- 418 Kelly, J. T., and Wexler, A. S.: Thermodynamics of carbonates and hydrates related to
419 heterogeneous reactions involving mineral aerosol, *J. Geophys. Res.-Atmos.*, 110, D11201,
420 doi: 11210.11029/12004jd005583, 2005.
- 421 Koehler, K. A., Kreidenweis, S. M., DeMott, P. J., Petters, M. D., Prenni, A. J., and Carrico,
422 C. M.: Hygroscopicity and cloud droplet activation of mineral dust aerosol, *Geophys. Res.*
423 *Let.*, 36, L08805, doi: 08810.01029/02009gl037348, 2009.
- 424 Krieger, U. K., Marcolli, C., and Reid, J. P.: Exploring the complexity of aerosol particle
425 properties and processes using single particle techniques, *Chem. Soc. Rev.*, 41, 6631-6662,
426 2012.
- 427 Laskin, A., Iedema, M. J., Ichkovich, A., Graber, E. R., Taraniuk, I., and Rudich, Y.: Direct
428 Observation of Completely Processed Calcium Carbonate Dust Particles, *Faraday Discuss.*,
429 130, 453-468, 2005.
- 430 Lee, A. K. Y., Ling, T. Y., and Chan, C. K.: Understanding hygroscopic growth and phase
431 transformation of aerosols using single particle Raman spectroscopy in an electrodynamic
432 balance, *Faraday Discuss.*, 137, 245-263, 2008.
- 433 Lei, T., Zuend, A., Wang, W. G., Zhang, Y. H., and Ge, M. F.: Hygroscopicity of organic
434 compounds from biomass burning and their influence on the water uptake of mixed organic
435 ammonium sulfate aerosols, *Atmos. Chem. Phys.*, 14, 11165-11183, 2014.
- 436 Liu, P. F., Li, Y. J., Wang, Y., Gilles, M. K., Zaveri, R. A., Bertram, A. K., and Martin, S. T.:
437 Lability of secondary organic particulate matter, *Proc. Natl. Acad. Sci. U. S. A.*, 113, 12643-
438 12648, 2016.
- 439 Ma, Q. X., He, H., and Liu, Y. C.: In Situ DRIFTS Study of Hygroscopic Behavior of
440 Mineral Aerosol, *J. Environ. Sci.*, 22, 555-560, 2010a.
- 441 Ma, Q. X., Liu, Y. C., and He, H.: The Utilization of Physisorption Analyzer for Studying the
442 Hygroscopic Properties of Atmospheric Relevant Particles, *J. Phys. Chem. A*, 114, 4232-
443 4237, 2010b.
- 444 Ma, Q. X., Liu, Y. C., Liu, C., and He, H.: Heterogeneous Reaction of Acetic Acid on MgO,
445 α -Al₂O₃, and CaCO₃ and the Effect on the Hygroscopic Behavior of These Particles, *Phys.*
446 *Chem. Chem. Phys.*, 14, 8403-8409, 2012.
- 447 Martin, S. T.: Phase transitions of aqueous atmospheric particles, *Chem. Rev.*, 100, 3403-
448 3453, 2000.
- 449 McFiggans, G., Artaxo, P., Baltensperger, U., Coe, H., Facchini, M. C., Feingold, G., Fuzzi,
450 S., Gysel, M., Laaksonen, A., Lohmann, U., Mentel, T. F., Murphy, D. M., O'Dowd, C. D.,
451 Snider, J. R., and Weingartner, E.: The effect of physical and chemical aerosol properties on
452 warm cloud droplet activation, *Atmos. Chem. Phys.*, 6, 2593-2649, 2006.
- 453 Pöschl, U.: Atmospheric Aerosols: Composition, Transformation, Climate and Health
454 Effects, *Angew. Chem.-Int. Edit.*, 44, 7520-7540, 2005.
- 455 Petters, M. D., and Kreidenweis, S. M.: A single parameter representation of hygroscopic
456 growth and cloud condensation nucleus activity, *Atmos. Chem. Phys.*, 7, 1961-1971, 2007.
- 457 Pope, F. D.: Pollen grains are efficient cloud condensation nuclei, *Environ. Res. Lett.*, 5,
458 044015, 2010.
- 459 Pruppacher, H. R., and Klett, J. D.: *Microphysics of Clouds and Precipitation* Kluwer
460 Academic Publishers, Dordrecht, Netherlands 1994.



- 461 Robinson, C. B., Schill, G. P., Zarzana, K. J., and Tolbert, M. A.: Impact of Organic Coating
462 on Optical Growth of Ammonium Sulfate Particles, *Environ. Sci. Technol.*, 47, 13339-13346,
463 2013.
- 464 Rubasinghege, G., and Grassian, V. H.: Role(s) of Adsorbed Water in the Surface Chemistry
465 of Environmental Interfaces, *Chem. Commun.*, 49, 3071-3094, 2013.
- 466 Schroeder, J. R., and Beyer, K. D.: Deliquescence Relative Humidities of Organic and
467 Inorganic Salts Important in the Atmosphere, *J. Phys. Chem. A*, 120, 9948-9957, 2016.
- 468 Schuttlefield, J., Al-Hosney, H., Zachariah, A., and Grassian, V. H.: Attenuated Total
469 Reflection Fourier Transform Infrared Spectroscopy to Investigate Water Uptake and Phase
470 Transitions in Atmospherically Relevant Particles, *Appl. Spectrosc.*, 61, 283-292, 2007a.
- 471 Schuttlefield, J. D., Cox, D., and Grassian, V. H.: An investigation of water uptake on clays
472 minerals using ATR-FTIR spectroscopy coupled with quartz crystal microbalance
473 measurements, *J. Geophys. Res.-Atmos.*, 112, D21303, doi: 21310.21029/22007JD008973,
474 2007b.
- 475 Seinfeld, J. H., and Pandis, S. N.: *Atmospheric Chemistry and Physics: From Air Pollution to*
476 *Climate Change*, Wiley Interscience, New York, 2006.
- 477 Sullivan, R. C., Moore, M. J. K., Petters, M. D., Kreidenweis, S. M., Roberts, G. C., and
478 Prather, K. A.: Timescale for Hygroscopic Conversion of Calcite Mineral Particles through
479 Heterogeneous Reaction with Nitric Acid, *Phys. Chem. Chem. Phys.*, 11, 7826-7837, 2009a.
- 480 Sullivan, R. C., Moore, M. J. K., Petters, M. D., Kreidenweis, S. M., Roberts, G. C., and
481 Prather, K. A.: Effect of Chemical Mixing State on the Hygroscopicity and Cloud Nucleation
482 Properties of Calcium Mineral Dust Particles, *Atmos. Chem. Phys.*, 9, 3303-3316, 2009b.
- 483 Swietlicki, E., Hansson, H. C., Hameri, K., Svenningsson, B., Massling, A., McFiggans, G.,
484 McMurry, P. H., Petaja, T., Tunved, P., Gysel, M., Topping, D., Weingartner, E.,
485 Baltensperger, U., Rissler, J., Wiedensohler, A., and Kulmala, M.: Hygroscopic properties of
486 submicrometer atmospheric aerosol particles measured with H-TDMA instruments in various
487 environments - a review, *Tellus Ser. B-Chem. Phys. Meteorol.*, 60, 432-469, 2008.
- 488 Tang, M. J., Whitehead, J., Davidson, N. M., Pope, F. D., Alfarra, M. R., McFiggans, G., and
489 Kalberer, M.: Cloud Condensation Nucleation Activities of Calcium Carbonate and its
490 Atmospheric Ageing Products, *Phys. Chem. Chem. Phys.*, 17, 32194-32203, 2015.
- 491 Tang, M. J., Cziczo, D. J., and Grassian, V. H.: Interactions of Water with Mineral Dust
492 Aerosol: Water Adsorption, Hygroscopicity, Cloud Condensation and Ice Nucleation, *Chem.*
493 *Rev.*, 116, 4205-4259, 2016.
- 494 Vali, G., DeMott, P. J., Möhler, O., and Whale, T. F.: Technical Note: A proposal for ice
495 nucleation terminology, *Atmos. Chem. Phys.*, 15, 10263-10270, 2015.
- 496 Veghte, D. P., and Freedman, M. A.: The Necessity of Microscopy to Characterize the
497 Optical Properties of Size-Selected, Nonspherical Aerosol Particles, *Anal. Chem.*, 84, 9101-
498 9108, 2012.
- 499 Vlasenko, A., Sjogren, S., Weingartner, E., Gaggeler, H. W., and Ammann, M.: Generation
500 of submicron Arizona test dust aerosol: Chemical and hygroscopic properties, *Aerosol Sci.*
501 *Technol.*, 39, 452-460, 2005.
- 502 Waguespack, L., and Hesse, N.: TN66: Humidity Calibration of Dynamic Vapor Sorption
503 (DVS) Instruments, TA Instruments, New Castle, DE 19720, USA, 2007.
- 504 Wexler, A. S., and Clegg, S. L.: Atmospheric aerosol models for systems including the ions
505 H^+ , NH_4^+ , Na^+ , SO_4^{2-} , NO_3^- , Cl^- , Br^- , and H_2O , *J. Geophys. Res.-Atmos*, 107, 4207, doi:
506 4210.1029/2001JD000451, 2002.
- 507 Wu, Z. J., Nowak, A., Poulain, L., Herrmann, H., and Wiedensohler, A.: Hygroscopic
508 behavior of atmospherically relevant water-soluble carboxylic salts and their influence on the
509 water uptake of ammonium sulfate, *Atmos. Chem. Phys.*, 11, 12617-12626, 2011.



- 510 Yeşilbaş, M., and Boily, J.-F.: Particle Size Controls on Water Adsorption and Condensation
511 Regimes at Mineral Surfaces, Scientific Reports, 6, 32136, doi: 32110.31038/srep32136,
512 2016.
513 Zhang, R. Y., Khalizov, A. F., Pagels, J., Zhang, D., Xue, H. X., and McMurry, P. H.:
514 Variability in morphology, hygroscopicity, and optical properties of soot aerosols during
515 atmospheric processing, Proc. Natl. Acad. Sci. U. S. A., 105, 10291-10296, 2008.
516